Energy Conversion and Management 337 (2025) 119904

Contents lists available at ScienceDirect

Energy Conversion and Management

journal homepage: www.elsevier.com/locate/enconman

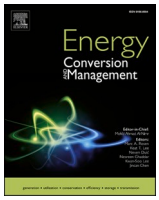

Absorption-enhanced Haber-Bosch for small-scale green NH_3 production. A feasibility study

Elvira Spatolisano *, Davide Figini

GASP - Group on Advanced Separation Processes & GAS Processing, Dipartimento di Chimica, Materiali e Ingegneria Chimica "G. Natta", Politecnico di Milano, Piazza Leonardo da Vinci 32, 20133 Milano, Italy

ARTICLE INFO

Keywords:
Green ammonia
Haber-Bosch process intensification
Distributed ammonia production
Decarbonization
Sustainable energy

ABSTRACT

In the context of energy transition, ammonia (NH_3), traditionally used as a fertilizer, represents a promising carbon-free energy vector due to its high hydrogen density (around 17.8 wt%). Nevertheless, the huge carbon intensity of NH_3 synthesis calls for an intensification of the conventional, fossil fuel-based Haber-Bosch process. Flexibility, small-scale plants, modularity and mild operating pressures become fundamental requirements for sustainable NH_3 production, obtained by green H_2 from water electrolysers. To achieve these objectives, this work presents a feasibility study for intensifying the Haber-Bosch process, performed by Aspen Plus® V14 simulation software. Lowering the operating pressure, the NH_3 condensation downstream the reactor is replaced by NH_3 absorption in water. Performances of the novel layout are assessed by means of an energy analysis, based on pinch technology and NH_3 equivalent method. Due to the lower power requirement than the traditional scheme and the absence of thermal energy requirement, the proposed configuration is proved to be a promising pathway towards sustainable and decentralized ammonia, supporting global efforts for transition to a low-carbon future.

1. Introduction

Ammonia (NH_3) is an important global commodity [1]: its production is around 175 million ton/y and it is expected to increase by 3–5 % in the coming years [2].

More than the 96 % of the current ammonia is obtained by the Haber-Bosch process which relies on fossil fuels (specifically, natural gas 50 %, oil 31 % and coal 19 % [3]) as feedstock for H_2 production via steam reforming, making it responsible for around 1.2 % of the total anthropogenic CO_2 emissions [3]. Decarbonizing NH_3 synthesis (*i.e.*, cutting down its associate CO_2 emissions) requires eliminating the reliance on fossil fuels in favour of renewable energy-powered electrolysis for green H_2 production [4].

Transitioning ammonia production to green energy sources presents significant challenges, primarily due to the intermittency of renewable energy and the difficulty in meeting the high energy demand of large-scale plants. Fossil fuels, by contrast, offer reliable availability and high energy density.

Adapting the Haber-Bosch process for such systems also involves addressing high operating pressures, which are essential for traditional setups but hinder the flexibility needed for renewable energy integration. Lowering operating pressures reduces conversion efficiency but enables quicker and safer plant start-up and shutdown cycles, making it more suitable for intermittent energy sources [5]. A balance must be struck between these two aspects.

To promote NH_3 formation as much as possible, research efforts are increasingly focused on new catalysts formulations and alternative ammonia separation methods [4,6]. As a matter of fact, lower-pressure operation necessitates improved NH_3 separation, achievable through *ex situ* (downstream) or *in situ* (within the reactor) removal, leveraging Le Châtelier's principle to enhance conversion [5]. Conventional condensation methods are impractical below 50 bar [4], leading to exploration of alternative approaches such as:

- Catalytic Membrane Reactors [6]. These integrate reaction and separation within a single unit. Options include reactant-permeable membranes and ammonia-permeable membranes [7]. Mainly computational studies are reported in literature, even if, recently, a first step towards the realization of an experimental apparatus was done [8]. While promising higher conversion rates and cost reductions are registered, challenges for technology implementation

* Corresponding author.
E-mail address: elvira.spatolisano@polimi.it (E. Spatolisano).

https://doi.org/10.1016/j.enconman.2025.119904
Received 28 February 2025; Received in revised form 28 April 2025; Accepted 5 May 2025
Available online 15 May 2025

include limited experimental data, the need for thermally stable membranes and insufficient selectivity for commercial purity.

- Adsorption. Alkaline metal halides (e.g., $CaCl_2$, $MgCl_2$) have shown high ammonia adsorption capacities [9]. Huberty et al. (2012) studied the kinetics of ammonia adsorption into $MgCl_2$ at the Haber-Bosch conditions [10]. Experimental setups were arranged for investigating the influence of adsorbent history, initial pressure, adsorber temperature and recycle flow rate. Afterwards, $CaCl_2$ was analysed [11,12]. Process optimizations were proposed, aiming to combine the reactor and the adsorber in a single piece of equipment, avoiding the recycle. New overall rate equations considering all the four resistances (in-out diffusion in the adsorbent, NH_3 reaction and adsorption) have been developed adopting a Fe-based catalyst with $NiCl_2$ and $MgCl_2$ adsorbents in a semi-batch reactor [13]. Automated systems that can control the adsorber temperature, pressure and flow rates revealed to be powerful tools for optimizing each reaction cycle [14]. The timing of heat transfer turns out to be crucial when operating with a large temperature difference between adsorption and desorption. Conversely, with a smaller temperature difference, the main limitation for adsorbent regeneration becomes the diffusion of the adsorbed molecules outside the pores of the supported metal halide [12,14]. Other sensitivity studies have been carried out on adopting reactor and adsorber separately or in a single unit [15]. However, operational complexities arise from PSA's discontinuous nature and adsorbent performance diminishes over cycles without support structures like silica [16,17].
- Absorption. Historically, ammonia absorption in water was used by BASF but abandoned due to limitations in refrigeration and catalyst poisoning by water vapor. Also, the resulting aqueous ammonia solution requires further distillation to produce pure liquid ammonia [18]. Snamprogetti reopened this possibility [19], eliminating the refrigeration cycle. Ammonia, synthesised at a pressure of 120 bar, was captured by a falling film absorber and then rectified to give liquid solution at 99.9 mol.%. The drying of the gas was assessed by injecting part of the liquid ammonia, whose evaporation caused a decrease in the temperature making the water condense and leaving only 1–3 ppm in the recycle. Experimental studies were conducted on the film absorber equipped with a cooling system [20] and maintained at a constant temperature of 40 °C [19]. A patent was filed in 1970 [21].

Other companies as Montecatini and Montedison (LEA Process) studied a layout of ammonia water absorption, where even a pressure of 65 bar was adopted in the synthesis loop [22]. In none of these instances, the layout was arranged to minimise the direct and indirect CO_2 emissions, neither attention was paid to its environmental sustainability.

The focus was to propose alternative NH_3 synthesis configurations, coupled with H_2 production from steam reforming, in huge production plants. Hot utility requirement was not an issue at that time.

Recent studies recalled the opportunity of absorption downstream the reaction section and proposed phosphate solutions for efficient ammonia recovery, achieving up to 99 % recovery with heat integration. This method offers potential for autothermal operation and cost reduction in small-scale setups. Nevertheless, when ammonia is chemically bonded with the solvent, a higher duty is required for the solvent regeneration.

On the other hand, water has a very good affinity with ammonia and a high relative volatility (the ratio between the vapor pressure of ammonia and the one of water is around 210 at 40 °C). For these two reasons, it was one of the most preferred solvents in cleaning NH_3-containing coke-oven gas [23].

Following the previous studies and in view of intensifying the Haber-Bosch process, this work proposes the integration of NH_3 absorption with water downstream the Haber-Bosch reactor, for the first time within the context of small-scale green ammonia plants. The process layout and operating conditions are arranged to minimize direct and indirect CO_2 emissions, to pave the way for a low carbon future. A base-case layout is presented and analysed. Then, process optimization is performed: by means of energy analysis, the configuration is made completely autothermal. Due to the lower power requirement than the traditional scheme and the absence of thermal energy requirement, the intensified Haber-Bosch is demonstrated to be worth-noticing for industrial applications.

Table 1
Basis of design for small scale green NH_3 production, based on [5].

Specification	Value
N_2 inlet flowrate [kmol/h]	298
H_2 inlet flowrate [kmol/h]	893
NH_3 production rate estimated [ton/d]	240
NH_3 purity [mol.%]	99.95
T_{in} [°C]	346

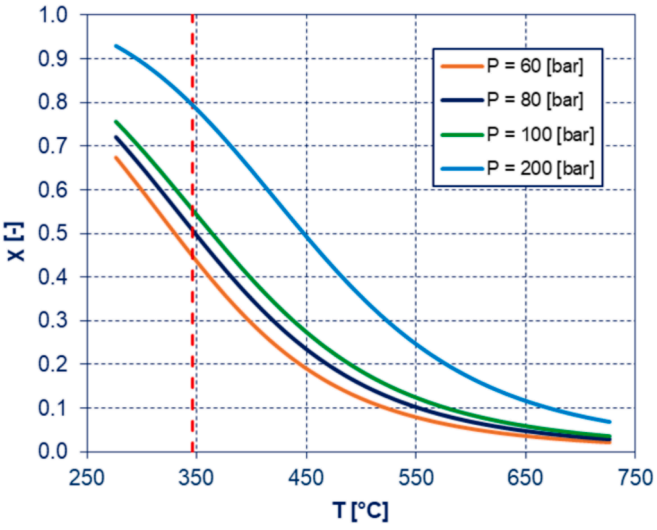

Fig. 1. N_2 equilibrium conversion (χ) as a function of temperature (T) at different pressures. N_2 is selected as the reference species to evaluate the conversion, being usually the slightly limiting reactant [5,26,27,28].

2. Haber-Bosch process intensification for green ammonia production

Table 1 summarises the basis of design for small-scale green NH_3 production. A realistic inlet hydrogen flow rate is estimated considering the electrolysers' productivity, together with the solar panels footprint. On the other hand, N_2 flowrate is fixed at roughly three times of the H_2 one. As a result, NH_3 production rate is evaluated, whose purity is specified in Table 1, as well. The high ammonia purity meets the standards of a wide range of industrial applications, as agriculture, refrigeration, electronics, and metallurgy.

The reactants' inlet temperature, considering Fe-based catalyst requirements, is equal to 346 °C [5]. While, regarding the pressure, the necessity of moving towards a small-scale production suggests the need for lower values. This is against the thermodynamics of the reaction (1). Common Haber-Bosch industrial plants operates within a pressure range of 100–250 bar [24]. Taking into account the N_2 equilibrium conversion of Fig. 1, pressures in between 60 and 100 bar are considered for reaction (1). The upper limit (100 bar) is the current lowest threshold of the conventional Haber-Bosch plant: Fe-based catalyst are able to efficiently operate at a minimum pressure of 90–100 bar [4,25]. The lower limit (60 bar) represents a trade-off between the thermodynamic limitation of ammonia reaction and the new process requirements: while low pressure is desirable for small-scale production, Fig. 1 indicates that

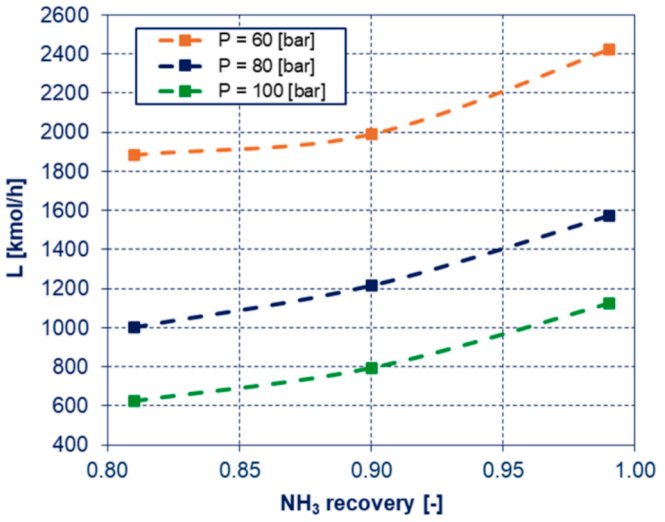

Fig. 2. Water demand (*L*) as a function of the NH_3 recovery at variable operating pressures of the absorption column.

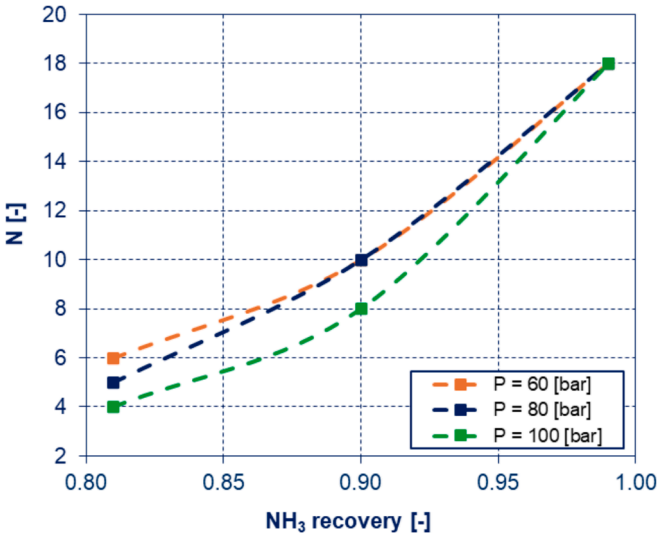

Fig. 3. Number of stages (*N*) as a function of the NH_3 recovery at variable operating pressures of the absorption column.

conversion will suffers significantly. Furthermore, high pressure is beneficial for the absorption process. Reducing the pressure further will not only hinder the separation performance, but also necessitates a higher amount of solvent.

$$3H_2 + N_2 \leftrightarrow 2NH_3 \Delta H_r(298.15[K]) = -45898[kJ/kmol_{N_2}] \quad (1)$$

The success of the new green NH_3 layout is based on outperforming a scaled-down version of the traditional Haber-Bosch process in terms of energy efficiency and consumptions. Therefore, for a fair comparison, the small-scale conventional Haber-Bosch process must be analysed and compared with the new absorption-enhanced configuration.

Details of the small-scale conventional Haber-Bosch layout are reported in the **supplemental material**, while the novel absorption-enhanced configuration is presented in the following section.

2.1. *Absorption-enhanced Haber-Bosch process*

In the absorption-enhanced Haber-Bosch process, the NH_3 condensation of the conventional layout is replaced with NH_3 absorption in water: downstream the reaction, the gas enters the absorber where ammonia is transferred from the gas phase to the liquid phase. The so-formed rich solvent is sent to the regeneration column for NH_3 separation and solvent recycle.

Alongside the three pressure levels 60, 80 and 100 bar (the operating pressure of the absorber is roughly the same of the reactor), an additional degree of freedom must be saturated for the absorption-based Haber-Bosch process, which is the ammonia recovery achieved at fixed solvent flowrate, defined as in equation (2).

$$NH_3 recovery = \frac{F_{NH_3} absorbed in water}{F_{NH_3} entering the absorber} \quad (2)$$

The performance of the reactor and absorber are closely interdependent. Lower ammonia recovery reduces water consumption, making regeneration less energy-intensive; however, this negatively affects reactor conversion·NH_3 recovery values of 0.81, 0.90 and 0.99 are chosen as they represent realistic scenarios for industrial applications.

To have an idea of the system's performance at fixed NH_3 recovery and, particularly, to set reliable values during the process simulation, a short-cut design problem is solved considering an operating temperature of 40 °C and a variable operating pressure (*i.e.*, 60, 80, 100 bar) for the absorption column. The minimum solvent flowrate required to achieve the fixed recovery is evaluated and then increased by the Kremser-Brown absorption factor range of 1.25–2 [29]. Known the solvent flowrate, the number of stages is calculated through the Kremser method. Results for this preliminary assessment are reported in Fig. 2 and Fig. 3, respectively.

As expected, a higher NH_3 recovery calls for higher solvent flowrate and more stages. The solvent flow rate is significantly affected by the operating pressure of the column. On the other hand, pressure has a lower impact on the number of stages: 20 stages seem to be adequate for the absorption column, regardless the pressure and NH_3 recovery.

Once NH_3 is absorbed in water, the rich solvent must be regenerated for enabling NH_3 separation and solvent recycle. To this aim, a conventional binary distillation column is introduced. As done for the absorber, a short-cut design problem is solved preliminary to the process simulation in Aspen Plus® V14.

At high recovery and low pressure, more water is needed at the absorber, causing the feed mixture at the regeneration unit to be more diluted (lower NH_3 molar fraction z_F, see Fig. 4b).

The distillation column operating pressure is set considering a dew point temperature of the top vapour product of 40 °C. This allows cooling water to be used as the cold utility. A value of 14 bar is thus calculated.

The three degrees of freedom of the distillation unit are fixed considering: NH_3 purity in the distillate equal to 99.95 mol.%, NH_3 recovery in distillate of 0.99 and a multiplicative constant of the minimum reflux ratio equal to 1.3.

Results from the short-cut design problem are reported in Fig. 4a, while Fig. 4b provides the relationship between the NH_3 molar fraction in the feed stream (z_F) and the NH_3 recovery in the absorption column.

Following the short-cut calculations, the absorption-enhanced Haber-Bosch process is simulated in Aspen Plus® V14, to analyse its performance.

To verify the reliability of the simulation software in representing the ammonia synthesis process, an existing industrial ammonia plant was modelled [5,26]. The results were compared with data available in the literature, demonstrating very good agreement between the Aspen Plus simulations and the performance of the real industrial plant.

As for the present case-study, the flowsheet of the process simulation is reported in Fig. 5. For simulation purposes, Redlich-Kwong-Soave equation of state with the Boston Mathias modification for the alpha function (RKS-BM) is selected to represent the system's thermodynamics. Pressure drops for heat exchangers were assumed to be 0.3 bar [29]. The process flow diagram of Fig. 5 can be distinguished into different sections, each one described in the following.

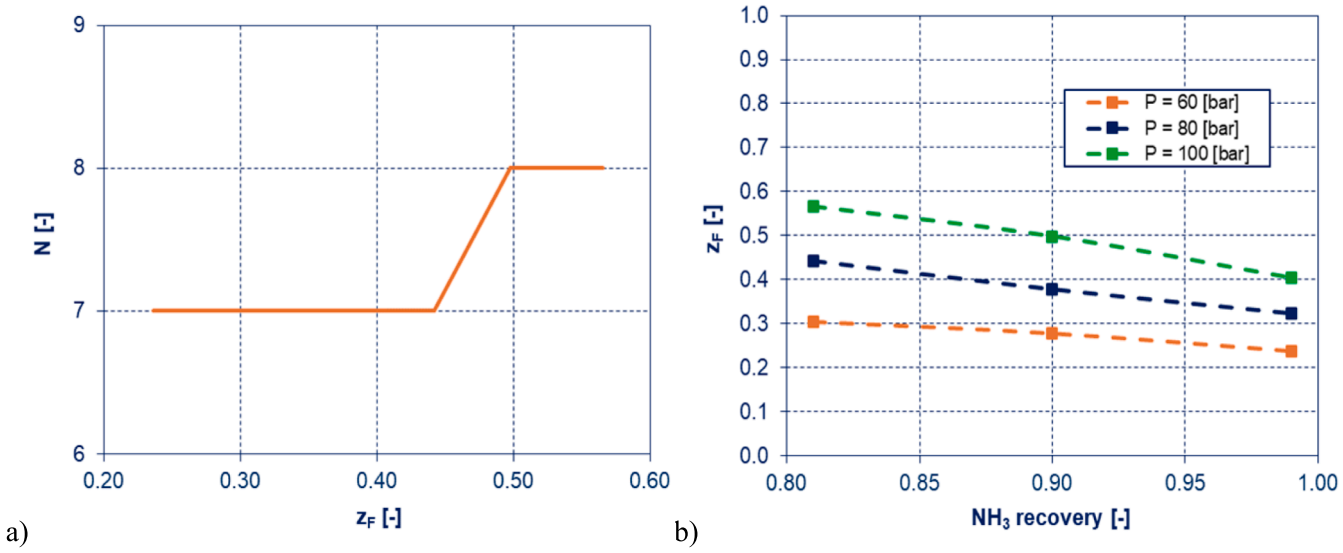

Fig. 4. A) number of stages (*N*) as a function of the feed mixture NH_3 molar fraction z_F; b) relationship between z_F and NH_3 recovery in the absorption column, at variable operating pressures of the absorption column.

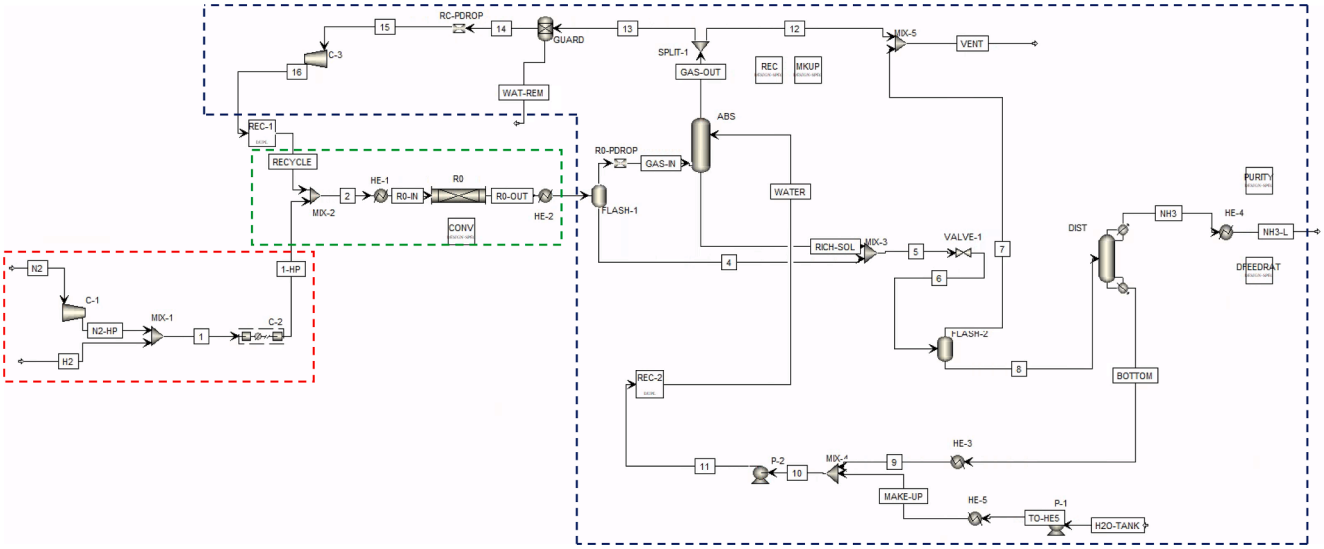

Fig. 5. Absorption-enhanced small-scale Haber-Bosch plant. Simulation in Aspen Plus® V14. In red: reactants' compression section; in green: reaction section; in blue: separation section. (For interpretation of the references to colour in this figure legend, the reader is referred to the web version of this article.)

Table 2
Catalyst's main features [25,26,28,31].

variable	value
d_p [mm]	5.7
density [kg/m^3]	3250
bed void fraction ε [-]	0.46

- Reactants' compression section (dashed in red in Fig. 5), required for the inlet H_2 and N_2 to reach the operating synthesis pressure. In this section, a multistage compressor with intermediate cooling is considered (*C-2* in Fig. 5).
- Reaction section (dashed in green in Fig. 5), in which NH_3 production occurs. To avoid superimposition of effects, single stage adiabatic reactor is considered at first (*R0* in Fig. 5). Then, the two-stage layout is investigated.

The reactor is sized using the Nielsen's correlation [5,26] and assuming about the 80 % of the equilibrium conversion for retrieving the catalyst volume [30]. *L/D* ratio of the plug flow reactor is fixed at 3 [5,30]. Reactor pressure drops are accounted through the Ergun equation, considering the catalyst equivalent particle diameter (d_p) and the density [28] as in Table 2.

The reaction exothermicity is exploited for reactants' pre-heating in a process-process heat exchanger (*HE-1* and *HE-2* in Fig. 5). Due to the thermodynamic limitations of reaction (1), per-pass conversion is low and unreacted N_2 and H_2 have to be recycled back, while NH_3 must be separated to be recovered in liquid phase.

- Separation section (dashed in blue in Fig. 5), which is the key distinction of this novel NH_3 synthesis layout with respect to the traditional one. The exiting gas stream from the reactor (*R0-OUT* in Fig. 5) is cooled down to 40 °C into *HE-2* and enters *FLASH-1*, to safeguard against traces of condensable gases. Then, the gas mixture enters the absorber, where it is counter-currently contacted with water to enable NH_3 separation. The NH_3 free gas, after dehydration

Table 3
Inlet and outlet streams specifications for the process of Fig. 5, together with the circulating water flowrate.

stream name		H2	N2	NH3	60 bar Water	80 bar Water	100 bar Water
		Inlet H_2	*Inlet N_2*	*NH_3 product*	*circulating solvent*	*circulating solvent*	*circulating solvent*
T	[°C]	25	30	35.5	40	41	41
P	[bar]	20	8	13.7	58	78	98
molar fractions							
N_2		0	1	0	0	0	0
H_2		1	0	0	0	0	0
NH_3		0	0	1	0	0	0
H_2O		0	0	0	1	1	1
F_{TOT}	[kmol/h]	892.91	301.62	593	1735.22	1354.75	1116.03

Table 4
Heating requirements, together with relating temperatures and utilities, for the process of Fig. 5.

equipment	60 bar			80 bar			100 bar			
	T_{in} [°C]	T_{out} [°C]	Q [kW]	T_{in} [°C]	T_{out} [°C]	Q [kW]	T_{in} [°C]	T_{out} [°C]	Q [kW]	*utility*
regeneration column reboiler	192.24	193.94	10933.05	191.85	193.85	9489.00	190.46	193.35	8186.38	MP steam

Table 5
Power requirements for the process of Fig. 5.

equipment	60 bar			80 bar			100 bar		
	P_{IN} [bara]	P_{OUT} [bara]	W [kW]	P_{IN} [bara]	P_{OUT} [bara]	W [kW]	P_{IN} [bara]	P_{OUT} [bara]	W [kW]
N_2 compressor	8	20	277.99	8	20	277.99	8	20	277.99
STAGE 1 + STAGE 2	20	60	1668.68	20	80	1999.68	20	100	2359.52
RECYCLE COMPRESSOR	56	60	699.79	76	80	474.89	96	100	352.12
LEAN PUMP	13.7	58	69.61	13.7	78	82.79	13.7	98	93.35

into a PSA unit (*GUARD* in Fig. 5) is recompressed to the reaction pressure and recycled back to the reactor. The NH_3 rich solvent outlet from the absorption column must undergo regeneration. To achieve this, *VALVE-1* reduces the stream pressure to 14 bar, the operating pressure of the distillation column. Any dissolved incondensable gas, such as N_2 and H_2, is removed in *FLASH-2* and subsequently vented. At the top of the downstream distillation column *DIST*, liquid ammonia is recovered, while the water stream at the bottom is cooled to 40 °C and pumped back to the absorber. A make-up stream compensates for water losses incurred in the *GUARD* unit.

The absorber is modelled as a staged adiabatic column ($N = 20$ from the short-cut calculations) using a rate-based approach. The circulating solvent flowrate, for each operating pressure, is fixed as in Fig. 2 for NH_3 recovery of 0.9. The exothermicity of ammonia absorption causes a temperature rise: this is a self-limiting effect, where higher temperatures reduce absorption rates and increase solvent demand. The temperature of the gas and liquid streams entering the absorption unit is 40 °C, while the operating pressure of the column is kept constant at the value of the reaction section (*i.e.*, 60, 80 and 100 bar for the different cases analysed), minus 2 bar to consider pressure drops within the lines. The regeneration column is also modelled as a staged column ($N = 15$, to be conservative with respect to the short-cut calculations) using a rate-based approach. Key manipulated variables are the distillate-to-feed ratio and the reflux ratio, optimized to meet the design specifications (*i.e.*, NH_3 purity and recovery in the distillate).

Table 3 summarises inlet and outlet streams for the process of Fig. 5, together with the circulating water flowrate for each pressure analysed. In addition, Table 4 and Table 5 provide, respectively, the heating and power requirements. All cooling requirements, to be performed with cooling water as utility, are neglected.

The thermal energy requirement of this absorption-enhanced Haber-Bosch configuration is mostly due to the reboiler of the regeneration unit. Being the product specifications of the distillation unit fixed, almost constant temperatures of $T = 194$ °C and $T = 44$ °C are observed at the reboiler and at the condenser, respectively.

3. Methodology for the energy analysis

The performance of the novel absorption-enhanced Haber-Bosch process of Fig. 5 is assessed by means of an energy analysis. Results of this novel process configuration have been, then, compared with the traditional layout. Indeed, the conventional Haber-Bosch NH_3 synthesis is autothermal: no heating is required and only electric energy is consumed for NH_3 separation from the unconverted gas. For the novel scheme to be promising, coupling between process streams has to be optimized and low energy consumption must be achieved. To this aim, pinch technology is employed to guarantee energy efficiency by minimizing utility consumption.

To match hot process streams with cold process streams, a minimum temperature difference (ΔT_{min}) of 10 °C is assumed. The cascade diagram is drawn to calculate the net heat transferred across each temperature range ΔT_i, as in equation (3), where m is the mass flow rate of each stream to be cooled/heated, while cp is its heat capacity. Each temperature range ΔT_i is identified knowing the initial and final temperature for all the streams to be heated/cooled.

$$\dot{Q}_i = \left[\sum_{i=1}^{NHS} (m \bullet cp)_{hot,i} - \sum_{i=1}^{NCS} (m \bullet cp)_{cold,i} \right] \bullet \Delta T_i [kW] \quad (3)$$

This diagram allows for the pinch temperature (T_{pinch}) identification, *i.e.*, the point in which the heat cascade hits zero value.

Composite curves are also drawn, which aggregate hot and cold streams based on their cumulative enthalpy (H), using a reference state where enthalpy is set to zero (typically the lowest temperature of the hot streams). For the cold composite curve, the minimum heat that must be added by an external utility is added at the lowest temperature. On the

Table 6
Cold utility requirements for the conventional Haber-Bosch process.

P [bar]	Cold utility requirement by cooling water [kW]	Cold utility requirement by refrigeration cycle [kW]
60	7039	6929 (81 + 6848)
80	7570	5756 (88 + 5668)
100	8794	4973 (99 + 4874)

other hand, for the hot composite curve, the minimum heat that must be removed (cooling utility) is found at the highest temperature. Both curves are then plotted on a *T-H* diagram to visually represent the energy demands and recovery potential.

To further refine the analysis, the grand composite curve (GCC) is developed by shifting the composite curves by half ΔT_{min} and calculating the enthalpy differences at each temperature level. The GCC provides a clear visualization of optimal utility demands across the system.

As a result, the optimal Heat Exchanger Network (HEN) is designed by coupling streams while avoiding temperature crossing.

For simplicity, counter-current heat exchangers are assumed throughout the network.

Optimized the process streams coupling following the well-established pinch methodology, the NH_3 equivalent method is applied to evaluate and compare energy consumption of the different process configurations. This method, adapted from the CH_4 equivalent analysis [32], allows for the summation of diverse energy inputs by equating them to the combustion of an equivalent amount of ammonia. Given the growing trend of using ammonia as a fuel to reduce CO_2 emissions associated with methane combustion, this approach aligns with sustainable energy goals.

All energy inputs as hot and cold thermal loads and electricity are converted into equivalent ammonia consumption. Similarly, energy outputs (e.g., steam generated for turbine expansion) are expressed as

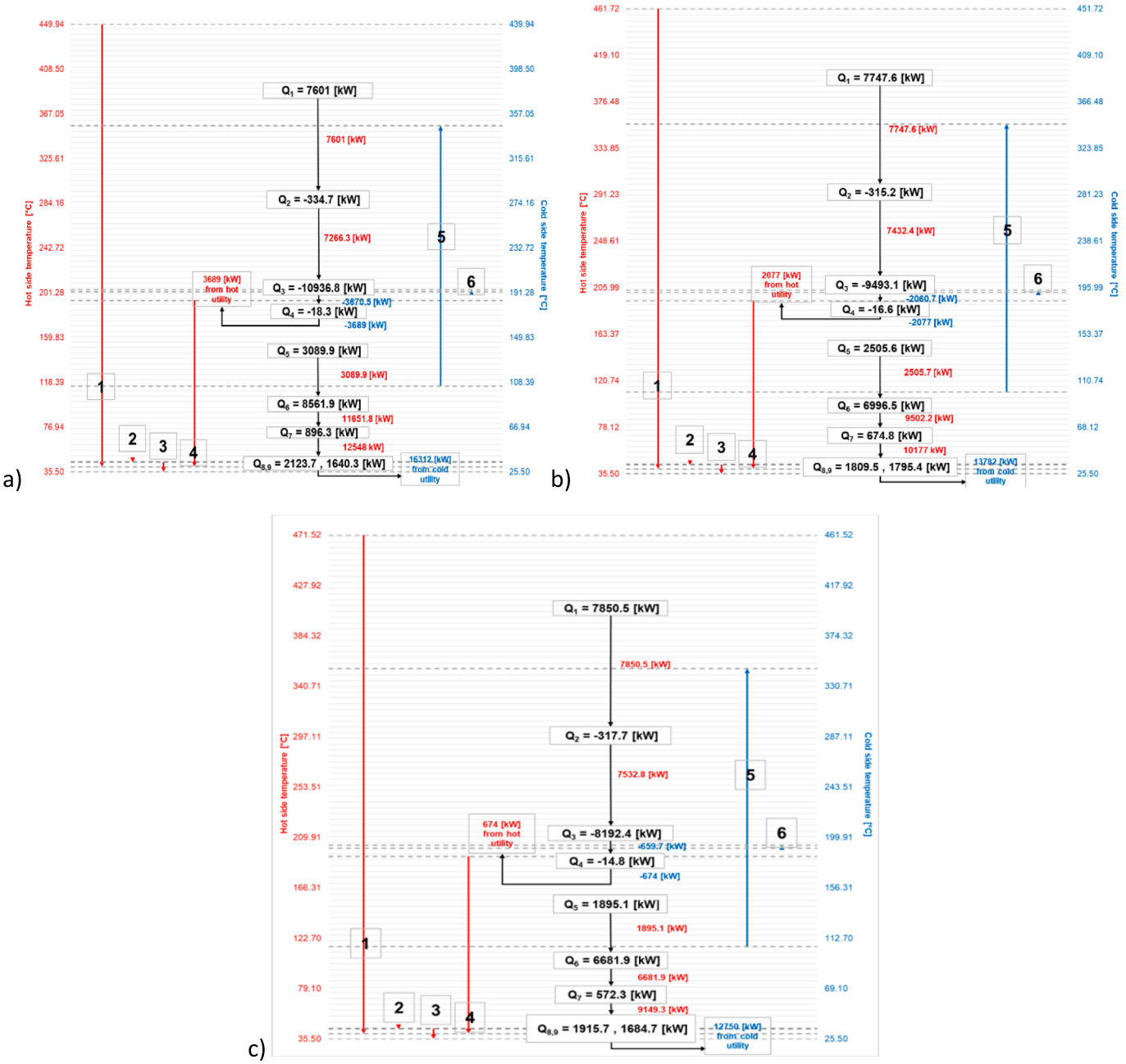

Fig. 6. Cascade diagram of the base-case absorption-enhanced Haber-Bosch process. a) $P = 60$ bar; b) $P = 80$ bar; c) $P = 100$ bar.

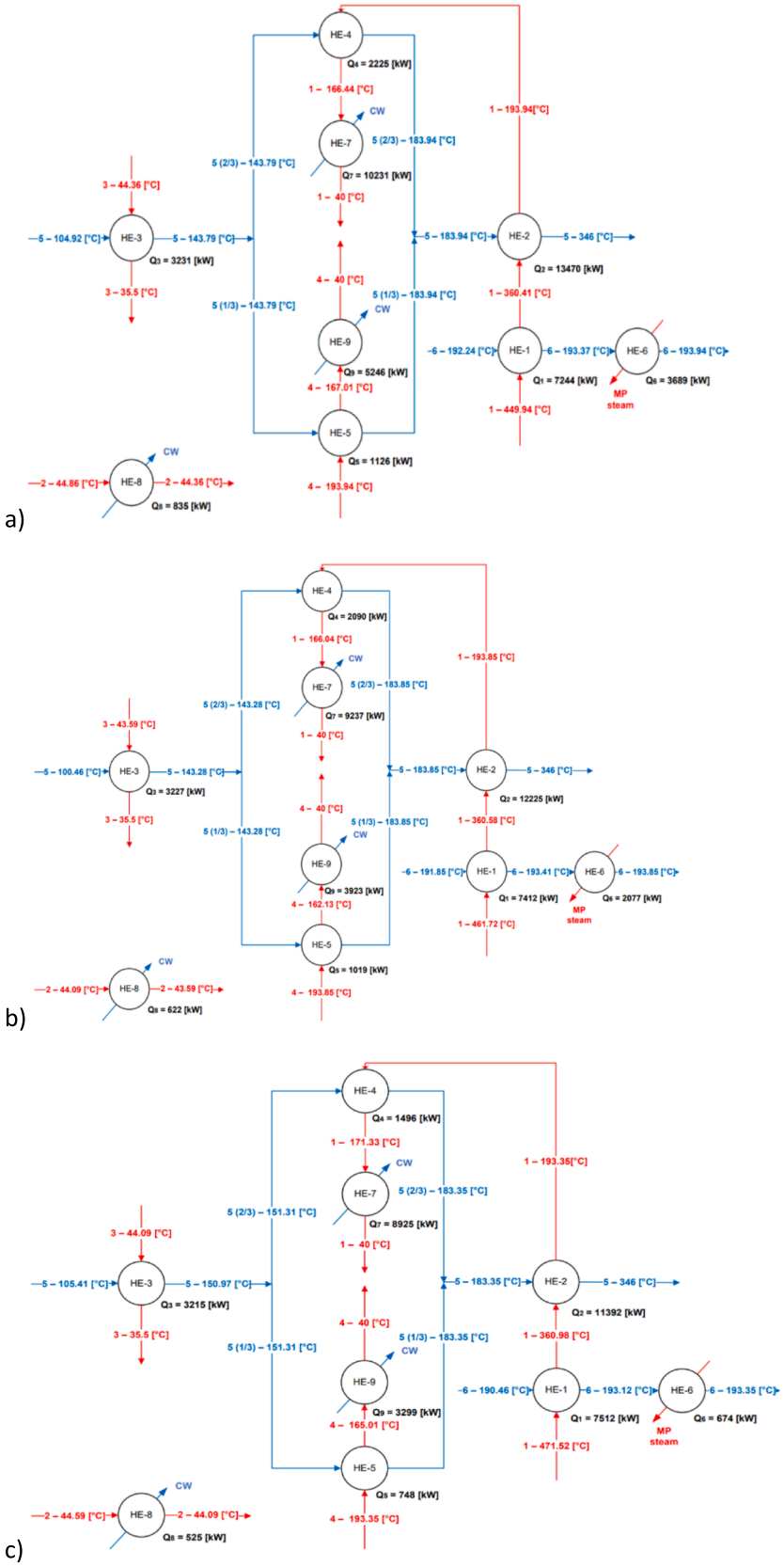

Fig. 7. Heat exchangers network of the base-case absorption-enhanced Haber-Bosch process. a) $P = 60$ bar; b) $P = 80$ bar; c) $P = 100$ bar.

Table 7
Streams' names in the HENs and Aspen Plus® V14 simulations. Absorption-enhanced Haber-Bosch process.

P [bar]	Streams' name in HENs	Streams' name in Aspen Plus® V14 simulation
60, 80, 100	1	*R0-OUT – 3*
	2	*DIST condenser inlet – NH3*
	3	*NH3 – NH3-L*
	4	*BOTTOM – 9*
	5	*2 – R0-IN*
	6	*DIST reboiler inlet – BOTTOM*

Table 8
Hot and cold utility requirements for the base-case absorption-enhanced Haber-Bosch process.

P [bar]	Cold utility requirement [kW]	Hot utility requirement [kW]
60	16,312	3689
80	13,782	2077
100	12,750	674

equivalent ammonia production. By convention, consumption is assumed positive, while production is supposed negative. For determining the net NH_3 requirement, contributions of energy consumption/production from process simulation are summed up, factoring in the efficiencies of each equipment unit ζ_i, and normalized by the NH_3 Lower Heating Value (LHV), roughly 316 MJ/kmol. This calculation provides the total NH_3 flow rate needed to power the process. The electric motor efficiency is set equal to 0.9, while the boiler efficiency for steam generation is assumed to be 0.8.

The NH_3 equivalent analysis incorporates a process efficiency parameter, ϕ, defined as in equation (4) and normalized by the NH_3 produced.

$$\phi = \sum_{i=1}^{NS} \frac{(energyconsorprod)_i \bullet \zeta_i}{(NH_3 produced) \bullet LHV_{NH_3}} [-] \quad (4)$$

This dimensionless parameter provides a robust metric for evaluating energy performance. The lower the value of ϕ, the better the energy performance of the process.

4. Results and discussion

Based on the methodology described in section 3, the energy performance of the novel absorption-enhanced Haber-Bosch is assessed and compared to the conventional process.

For the conventional Haber-Bosch process, all three pressure levels yield remarkably similar results, with almost identical predicted HENs (see the **supplemental material** for further details). The key distinction lies in the temperature profiles associated with the reactor conversion and the refrigeration cycle for each pressure level. The process achieves excellent heat integration by utilizing the exothermic reaction to eliminate the need for hot utilities. However, it does require a cold utility, which is to be provided by cooling water and by a refrigeration cycle for the remaining lower temperature needs (Table 6).

The refrigeration cycle is a crucial item because its compressor requires a non-negligible amount of electric energy.

On the other hand, Fig. 6 and Fig. 7 provide, respectively, the cascade diagram and the HEN of the base-case absorption-enhanced Haber-Bosch process for the three pressure levels analysed: $P = 60$ bar, $P = 80$ bar, $P = 100$ bar. The correspondence between stream numbers and Aspen Plus® V14 simulation streams names of Fig. 5 is outlined in Table 7.

As in the conventional Haber-Bosch case, the HENs exhibit the identical layout, with variations on the duties reflecting the pressure-dependent behaviour of the reaction. However, for the base-case absorption-enhanced Haber-Bosch process the hot utility demand is higher due to the need of a significant amount of steam at the regeneration column reboiler. Higher pressure operation leads to a decrease in hot utility demand. Conversely, cold utility requirements are entirely fulfilled by cooling water. Table 8 summarizes all the utility duties required for each pressure level.

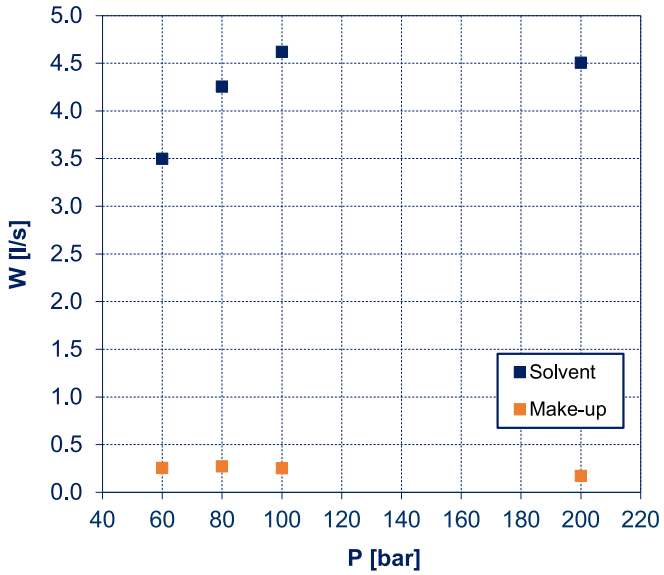

Fig. 8. Water flow rate (W) as a function of the operating pressure P for the autothermal absorption-enhanced Haber-Bosch process.

The heating requirement is the major drawback of the base-case layout. Indeed, the sustainable green NH_3 production becomes questionable if medium pressure steam is needed as utility, as its production is tied to CO_2 emissions. Therefore, an attempt is made to improve the energy balance of the plant, aiming to generate all necessary heat internally by optimizing the coupling of process streams.

The primary hot utility demand is found in the distillation column reboiler, responsible for the solvent regeneration and, thus, strictly related to the amount of water circulating in the plant. Reducing the water flowrate implies lower reboiler duty. However, decreasing the water flowrate also reduces NH_3 recovery in the absorber liquid phase, leading to a higher concentration of ammonia in the recycled gas stream. This shift would drive the reaction equilibrium back towards the reactants, further lowering the already low conversion due to the reduced operating pressure. Optimizing the absorption-enhanced Haber-Bosch process is, thus, challenging: if both autothermal behaviour and good process performance are required, a proper trade-off between all the process parameters must be identified. To do so, the constraint of 90 % of NH_3 recovery in the liquid phase outlet is removed, allowing for an assessment of the necessary water flowrate to ensure the configuration remains autothermal.

The autothermal behaviour of the configuration is proved by the pinch analysis, which allows to optimize the thermal coupling between process streams. Results for this optimization are reported in section 4.1.

4.1. Process optimization

Fig. 8 shows, for each operating pressure, the resulting circulating water flow rate, together with its make-up, to guarantee the autothermal behaviour. Around 3.5–4.5 L/s of water circulate within the plant, while the make-up flowrate remains always below 0.3 L/s.

Based on the water flow rate of Fig. 8, the Aspen Plus® V14 [33] process simulation is developed with the same logic of the base-case layout. Redlich-Kwong-Soave equation of state with the Boston

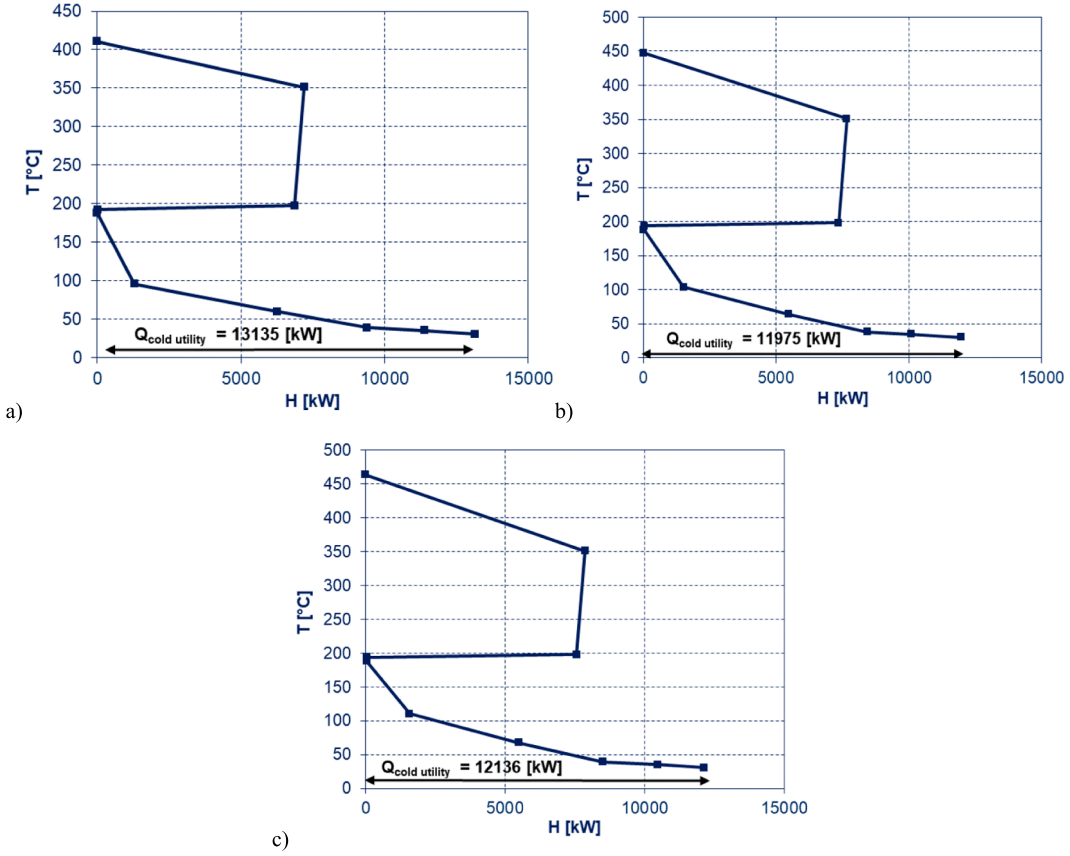

Fig. 9. Grand composite curve of the autothermal absorption-enhanced Haber-Bosch process. a) $P = 60$ bar; b) $P = 80$ bar; c) $P = 100$ bar.

Mathias modification for the alpha function (RKS-BM) was used to represent the system's thermodynamics. Pressure drops were considered to be 0.3 bar for heat exchangers [29]. Once again, the reactor is assumed as a single stage adiabatic plug flow, whose pressure drops are accounted for through the Ergun correlation.

To prove the autothermal behaviour of the whole configuration, Fig. 9 shows the grand composite curve for the different cases analysed ($P = 60$, 80 and 100 bar), while Fig. 10 provides the corresponding Heat Exchanger Network (HEN).

As can be observed from the comparison of the HENs of Fig. 10 with Fig. 7, results of the optimized layout are very similar to the base-case configuration at a fixed NH_3 recovery of 0.90. The only difference is the absence of the utility heat exchanger consuming MP steam (HE-6 in Fig. 7).

The hot utility requirements are all zero for each case analysed, as can be observed from the grand composite curves, while the cold utility requirement, to be provided with cooling water, are reported in Table 9.

As for the electric energy consumptions, the performance of the autothermal absorption-enhanced Haber-Bosch technology is reported in Fig. 11, and compared to the traditional layout (in Fig. 11, SbC stands for Separation by Condensation of the traditional Haber-Bosch). The power required for the different configurations is normalised with respect to the NH_3 produced.

This chart reveals that the refrigeration cycle compressor is the main source of energy consumption in the process. This translates into higher electricity requirements for the traditional layout compared to the new one. As expected, pumps contribute minimally to the overall energy consumption. The contribution of the recycle compressor is higher at lower pressures, because of the lower conversion achieved. The difference in the power demand between the two configurations decreases at increasing reaction pressure.

From the electric energy consumption point of view, the novel process seems very competitive: its electric energy consumption is significantly lower than the conventional one.

For the sake of completeness and in view of assessing the behaviour of the novel layout as a function of pressure, another pressure level, 200 bar, is considered, closer to the state-of-art pressure for NH_3 synthesis. Process simulation has been accomplished for both the traditional layout and the autothermal absorption-enhanced Haber-Bosch technology. Thermal and electric energy requirements have been retrieved from process simulation, to include these case-studies in Fig. 11 and Fig. 12, as well.

For a thorough comparison of the two alternatives, Fig. 12 summarises the results of the NH_3 equivalent analysis, based on the methodology recalled in section 3.

The novel absorption-enhanced configuration (blue in Fig. 12) shows a considerably lower energy demand at low pressures (around 80 bar), which is roughly half than the traditional one. This result opens the possibility of adopting water absorption in the framework of the Haber-Bosch process intensification. On the other hand, at higher pressure ϕ is comparable: this justifies the unfeasibility of adopting such a separation method in the common large-scale production operated at high pressure. In fact, at these process conditions, the complexity of the novel separation process exceeds the minimal energy gains.

A minimum trend for the ϕ parameter can be observed in Fig. 12. If pressure is shifted towards very low values, ϕ seems to approach a vertical asymptote. This represents the unfeasibility condition for this process, where reaction and separation are strongly limited: the absorber would consume a lot of water, such that it would be very difficult to keep the system autothermal because of the high regeneration duty. Conversely, at very high pressure, ϕ tends to increase since the reactants' compression will become more and more energy intensive, hiding the benefits obtained in the lower recycle flow rate. Also for the conventional process the vertical asymptote is expected at low

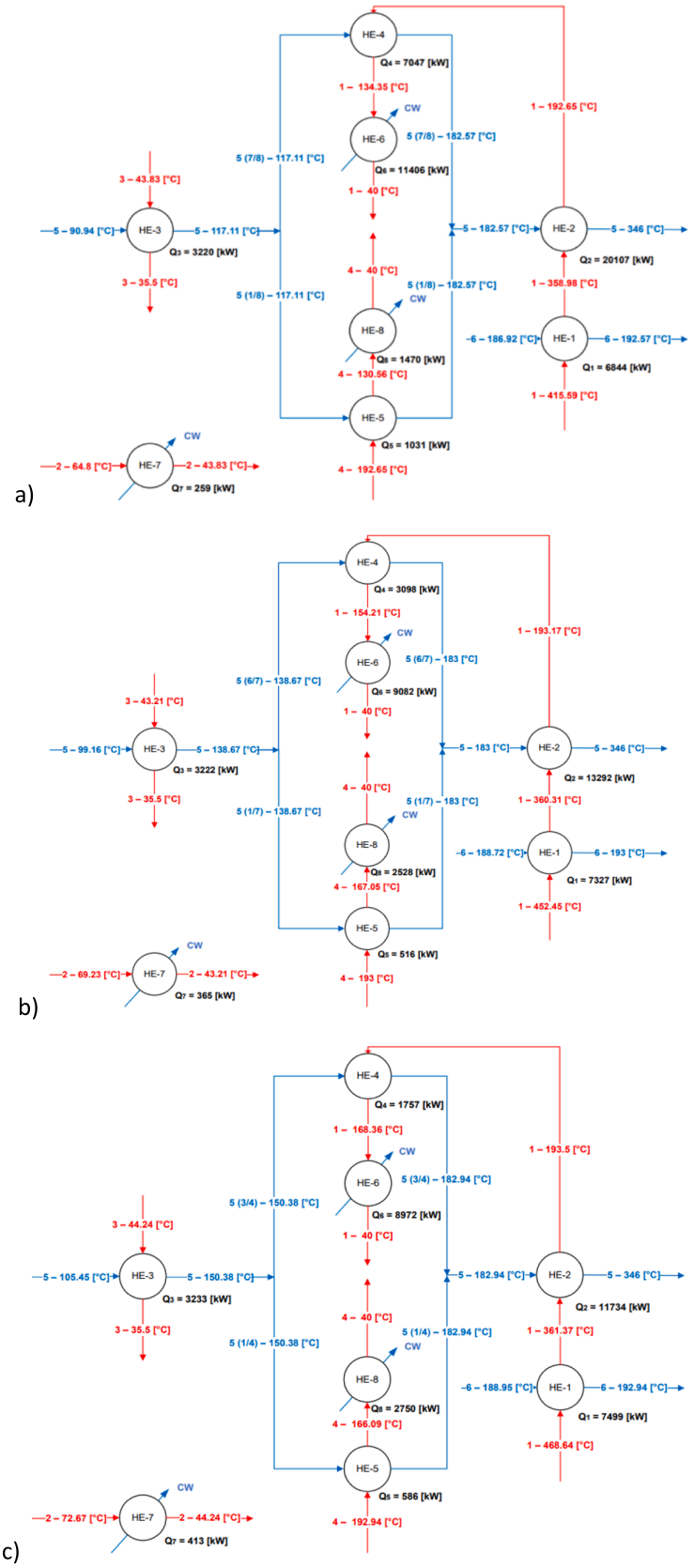

Fig. 10. Heat exchangers network of the autothermal absorption-enhanced Haber-Bosch process. a) $P = 60$ bar; b) $P = 80$ bar; c) $P = 100$ bar.

Table 9
Cold utility requirements of the autothermal absorption-enhanced Haber-Bosch process.

P [bar]	Cold utility requirement [kW]
60	13,135
80	11,975
100	12,136

pressures. Poor performances have been obtained for 60 bar case, in accordance with scientific literature claiming that the Haber-Bosch process is not feasible anymore at pressures below 50 bar.

For a critical analysis of the results of Fig. 12, Fig. 13 offers the dimensionless net equivalent NH_3 requirement (ϕ) as a function of the NH_3 recovery achieved in the separation section at different pressures, for both water absorption and condensation. For condensation as NH_3 separation method, also the theoretical allowable maximum is considered. This latter case assumes an ammonia-based refrigeration cycle operated at the lowest possible temperature [34] (*i.e.*, −40 °C) for all the pressure levels.

Fig. 13 shows that the novel autothermal process, starting from 80 bar, is able to guarantee comparable or even better NH_3 recoveries within the absorption column, keeping a lower energy consumption. The higher NH_3 recovery in the absorption column reduces the ammonia

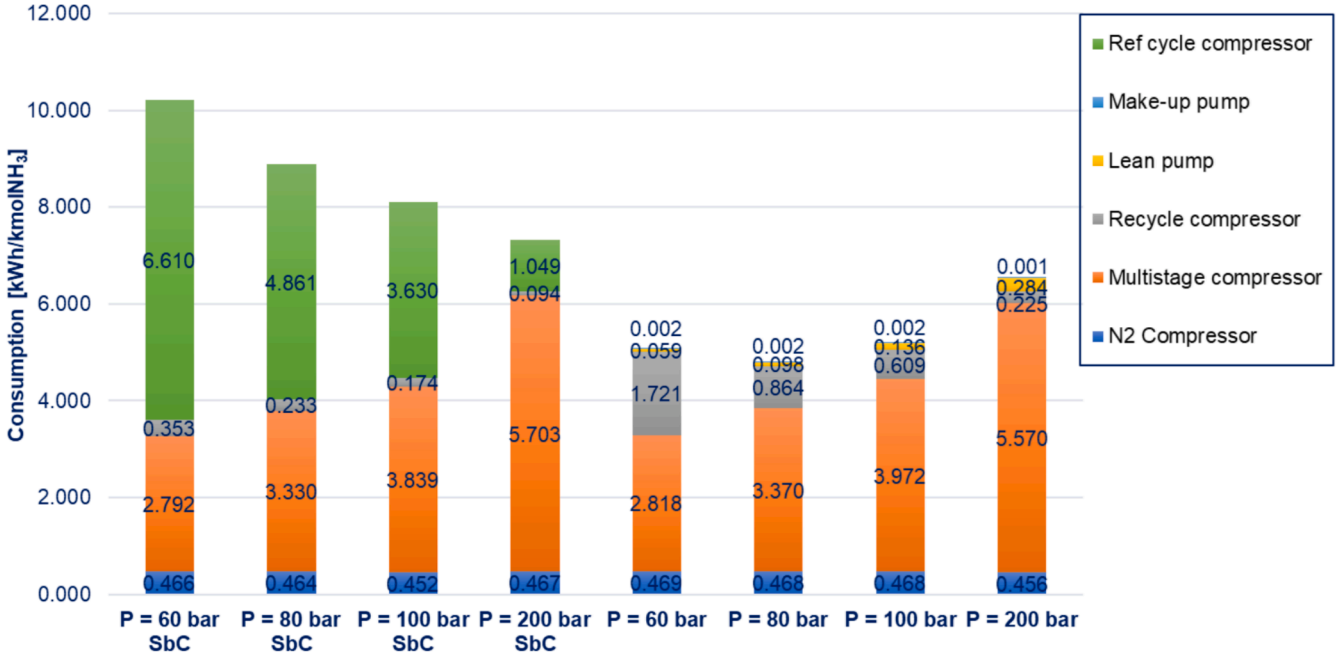

Fig. 11. Electric energy consumption: comparison between the traditional layout (SbC) and the autothermal absorption-enhanced Haber-Bosch process.

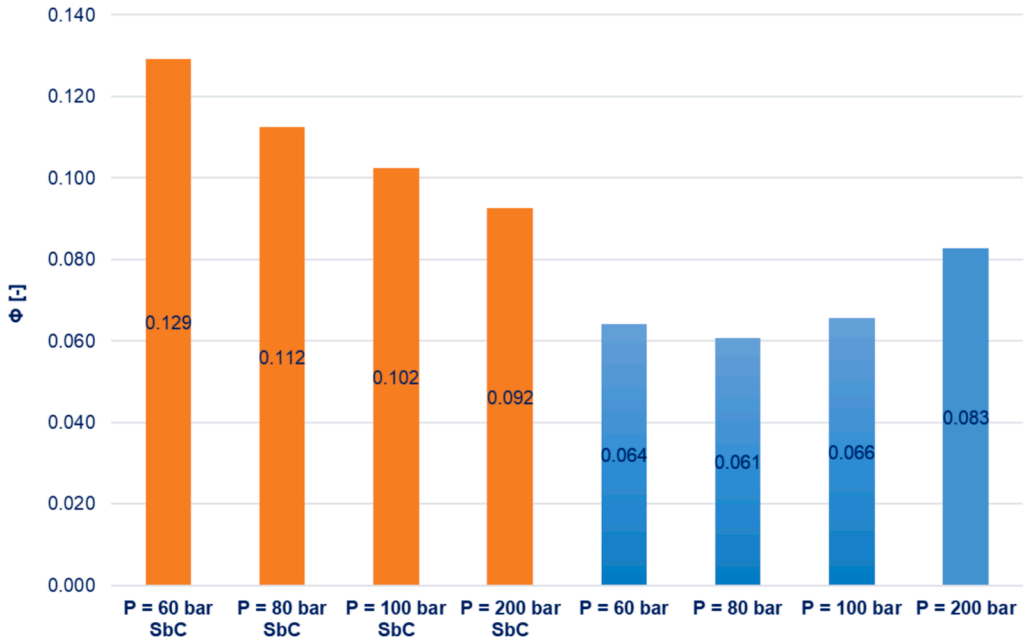

Fig. 12. Results of the NH_3 equivalent analysis for the conventional Haber-Bosch (orange) and the autothermal absorption-enhanced Haber-Bosch (blue). (For interpretation of the references to colour in this figure legend, the reader is referred to the web version of this article.)

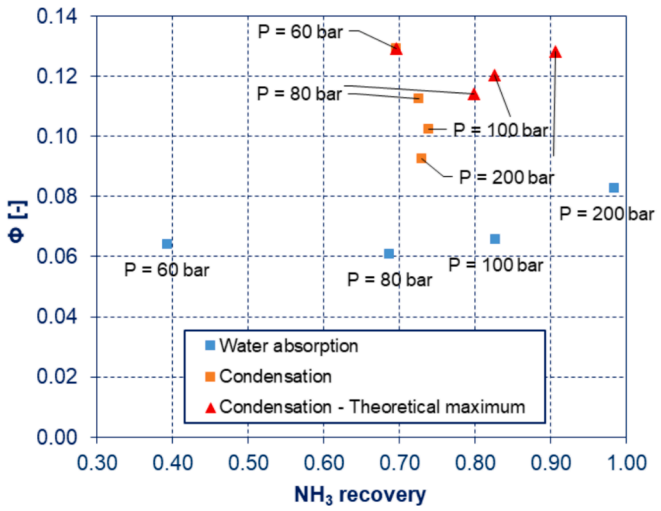

Fig. 13. Dimensionless net equivalent NH_3 requirement (ϕ) as a function of the NH_3 recovery achieved in the absorption section at different pressures, for both water absorption and condensation as NH_3 separation technologies.

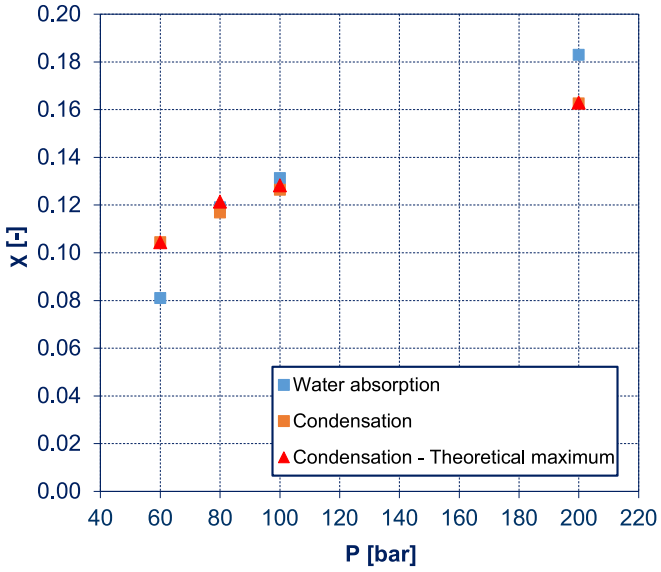

Fig. 14. N_2 conversion as a function of the NH_3 synthesis operating pressure, for all the process configurations analysed: separation by condensation and separation by NH_3 absorption.

content of the gas phase recycle and, thus, improves the conversion. Note that for 60 bar, the theoretical maximum is superimposed to the real case. However, as a general remark, for the theoretical maximum higher recovery are observed at the expenses of increasing ϕ.

Fig. 14 shows the N_2 conversion depending on the NH_3 synthesis operating pressure, for all the process configurations analysed (*i.e.*, separation by condensation and separation by NH_3 absorption).

As dictated from thermodynamics, higher pressures mean higher conversions.

Fig. 14 confirms that 80 bar scenario is the breakthrough point between the two configurations. At higher pressures, the autothermal absorption-enhanced Haber-Bosch shows higher nitrogen conversion than the traditional configuration, while at lower pressures a lower conversion is experienced. This is because of the poor separation performance achieved at 60 bar, responsible for a higher NH_3 content in the recycle stream. The opposite holds true for 200 bar.

To verify if conversion can be improved further in the case of the autothermal absorption-enhanced Haber-Bosch, the possibility of applying a two-stage reactor configuration is explored in section 4.2.

4.2. Two-stage layout

For the two-stage absorption-enhanced Haber-Bosch process, sizing of each reaction stage is required. The same methodology outlined in our previous work is applied to minimize the catalyst volume for each stage [5].

Sized the reaction stages, Aspen Plus® V14 simulation is carried out for the two pressure levels of this analysis (80 bar and 100 bar). Based on the results of process simulations for the absorption-enhanced Haber-Bosch process, Fig. 15 displays a comparison between single and the two-stage layout in terms of electricity consumption.

The absorption is assumed to be adiabatic in all the cases reported in Fig. 15.

As observed in Fig. 15, reactants compression is, in both cases (*i.e.*, single and two-stage reactor), the most energy-intensive operation. The difference between the two arrangements lies in the recycle compressor. Even though higher pressure drops are expected in the two-stage configuration, the higher conversion attained allows a much smaller recycle flowrate and, consequently, a reduced power demand. Since both the configurations are autothermal, the electric energy consumption is an indication of the overall energy demand of the process.

Due to low difference between the two configurations, it is not possible to firmly state that the two-stage layout is the optimal one. A comprehensive techno-economic assessment is needed, to evaluate CAPEX and OPEX and, thus, determining the best alternative.

The increase in the conversion granted by the two-stage enables to better exploit the reaction heat. Thus, a higher amount of water can be used as a solvent in the absorber, enabling a higher NH_3 recovery. This effect is much more evident at 80 bar, suggesting that at such a low pressure the two-stage might be the preferred choice.

The conversion, which is always higher at higher pressure, is almost doubled if two stages are employed, as depicted in Fig. 16.

To confirm that the proposed two-stage layout is less energy-intensive than the conventional two-stage ammonia synthesis loop, Fig. 17 shows the comparison in terms of electric energy consumptions between the conventional and the absorption-enhanced Haber-Bosch process.

The presence of the refrigeration cycle in the conventional Haber-Bosch layout (labelled as “SbC” – Separation by Condensation – in Fig. 17) is always the key element responsible for the higher electricity consumption. However, with a two-stage reactor, higher conversions can be reached and, thus, higher operating temperature can be employed during refrigeration. In this case, the higher conversion implies higher amount of heat released by the exothermic reaction.

The conventional two-stage process better behaves at 100 bar, which is the actual lowest threshold of the conventional plants. If lower operating pressures are required, the autothermal absorption-enhanced Haber-Bosch technology turns out to be a viable alternative for industrial application.

4.3. Further insights: Isothermal absorption

To further explore the potential of absorption-enhanced Haber-Bosch, the possibility of adopting an isothermal film absorber has been analysed for 80 bar and 100 bar two-stage case-studies [19]. Performing absorption adiabatically, a temperature increase is observed due to the exothermicity of operation (see Fig. 18). The peak of temperature profile is experienced in the vicinity of stage 4–5 (the stage numbering is top–bottom), where the solvent is still lean. This increase in temperature is self-inhibiting because absorption is favoured at low temperatures. Higher temperatures have a negative impact on NH_3 recovery and, to guarantee a fixed absorption performance, a higher amount of water is required by the adiabatic configuration. For this reason, isothermal

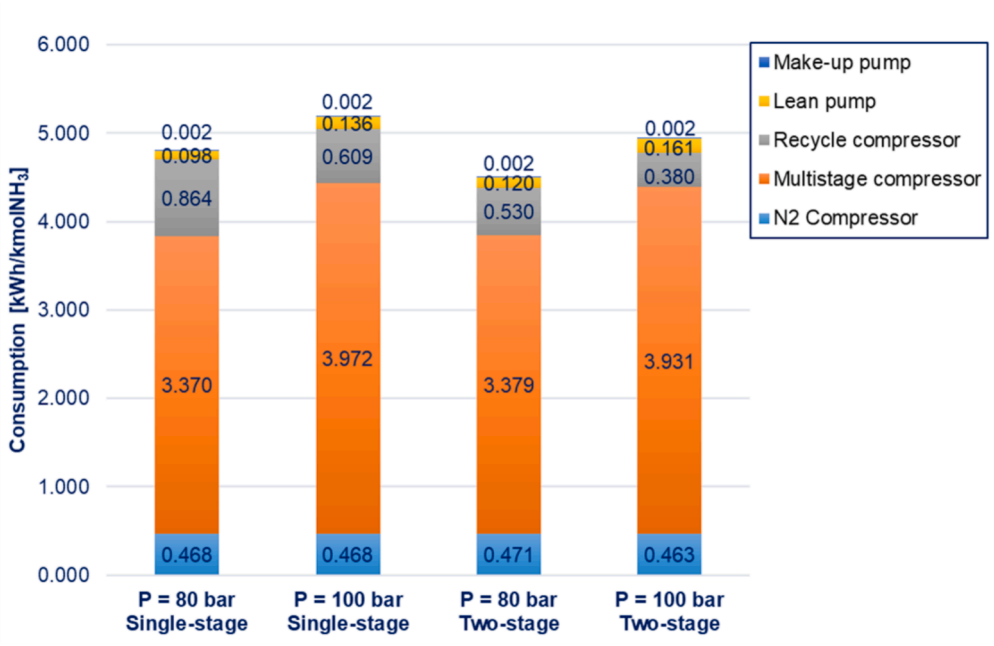

Fig. 15. Electric energy consumption of the autothermal absorption-enhanced Haber-Bosch process. Comparison between the single and two-stage layout.

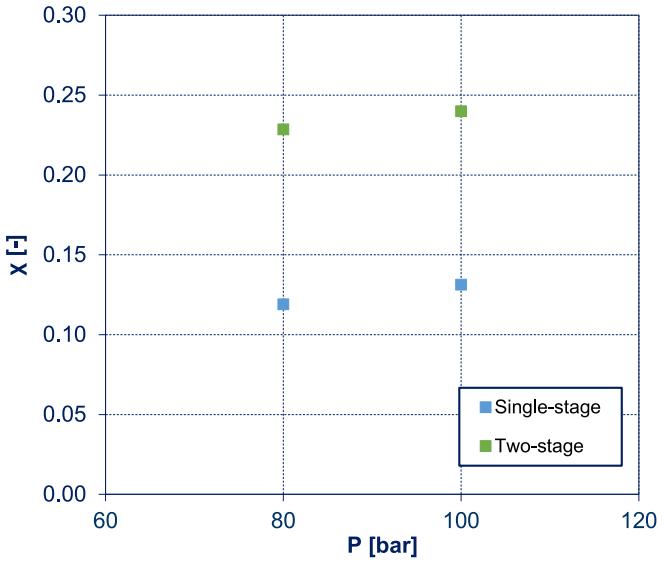

Fig. 16. N_2 conversion as a function of the NH_3 synthesis operating pressure (P) for autothermal absorption-enhanced Haber-Bosch. Comparison between the single stage and two-stage configuration.

absorption is worthy of investigation. In this case, a cooling medium is required to keep the temperature constant. For maintaining the absorber operating temperature at 40 °C (*i.e.*, the inlet temperature for both gas and liquid streams in the adiabatic configuration), cooling water is employed.

Considering that the primary focus of this analysis is the preliminary assessment of isothermal absorption, a simplified approach is adopted for simulation purposes. If results reveal that the isothermal absorber does not offer a significant energetic advantage over an adiabatic one, a detailed model will be unnecessary, and this configuration will be excluded from further investigation.

The isothermal absorber is implemented in Aspen Plus® V14 considering a side duty to be removed from the absorption column, in the vicinity of the temperature peak (a rigorous analysis should indicate the optimal position of this duty to be removed). A trial-and-error approach is adopted: the absorber must be run isothermally, but, meanwhile, the overall layout must preserve its autothermal behaviour. Autothermicity is achieved manipulating the water flow rate, which, in turn, affects the absorber's temperature.

Temperature profiles for the isothermal absorber are shown in Fig. 19.

Keeping a perfectly flat profile is difficult to be achieved according to the simplified methodology adopted. Nevertheless, the temperature difference between the minim and maximum value is limited to 20 °C.

Increasing the pressure from 80 to 100 bar, a higher average temperature is observed within the absorption column.

Gran composite curves of the absorption-enhanced Haber-Bosch are reported in Fig. 20, to prove the autothermal behaviour of the overall layout in the case of isothermal absorption, too, for both 80 and 100 bar. As it is possible to note in Fig. 20, a heat removal at high temperature is present, allowing for medium steam generation, eventually (temperature process-side is around 190 °C). This heat surplus is a consequence of the advantages of the isothermal absorption: the lower water demand allows the regeneration column reboiler to be less energy-demanding. This effect is more evident for 100 bar, as absorption is more favoured in this case. This enhanced performance is achieved at the expense of increased layout complexity and cooling water flowrate.

As a matter of fact, isothermal absorber requires a non-negligible amount of cooling water, evaluated considering that it enters the absorber at 25 °C and leaves the unit at 40 °C (around 50 L/s, depending on the operating pressure considered).

Even if promising, still uncertainties remain.

4.4. Comparison of the proposed process configurations

For the sake of completeness, Fig. 21 condenses all the configurations studied, considering single and two stage layout, variable operating pressure, adiabatic and isothermal absorber.

Fig. 21 clearly indicates that the single-stage absorption-enhanced Haber-Bosch significantly outperforms the benchmark for small-scale (*i.e.*, traditional Haber-Bosch operated at $P = 200$ bar), achieving energy savings of up to 37 % with isothermal absorption. However, the simpler design and comparable savings are observed for the adiabatic case. In

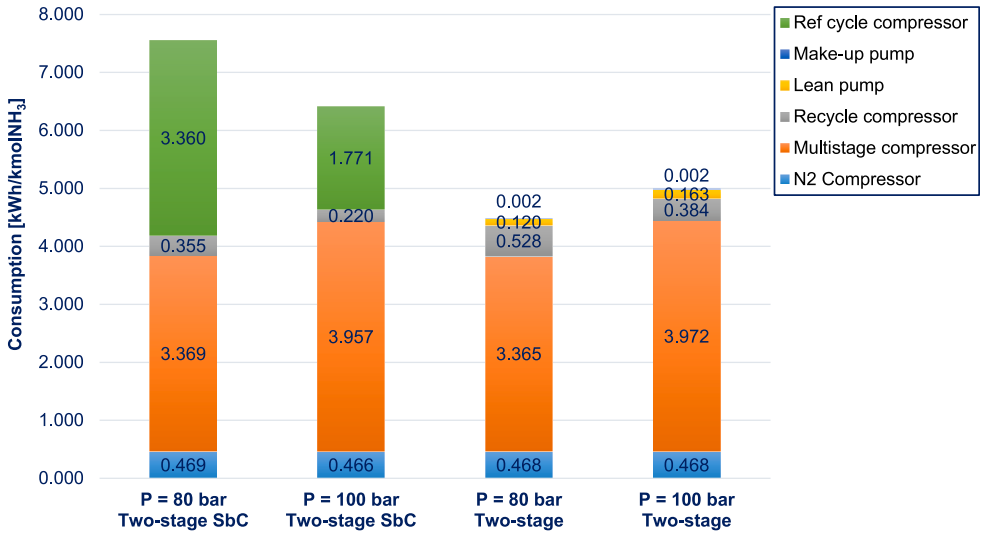

Fig. 17. Electric energy consumption. Comparison between the two-stage conventional and absorption-enhanced Haber-Bosch.

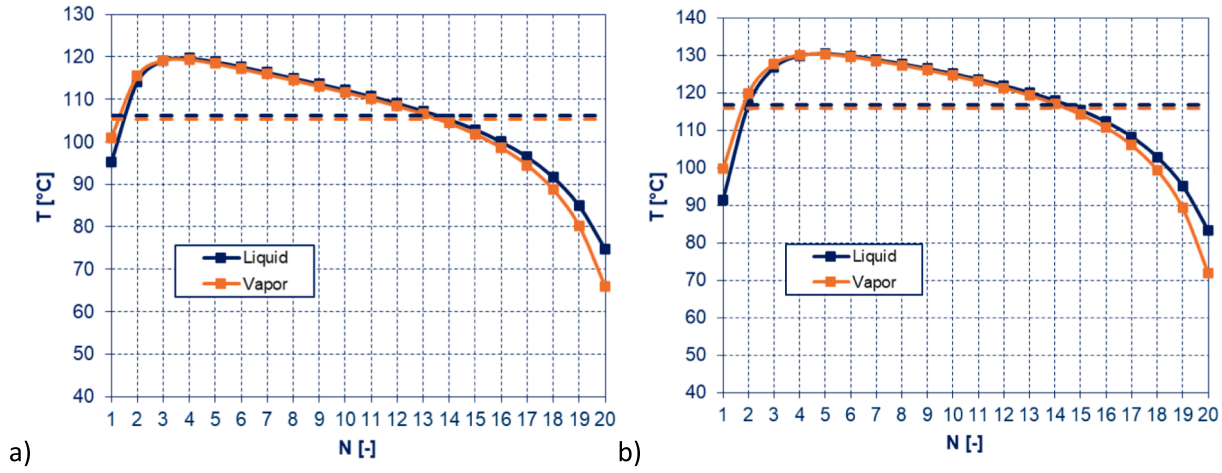

Fig. 18. Temperature profiles for the adiabatic absorber. a) $P = 80$ bar; b) $P = 100$ bar. The horizontal dashed lines represent the mean temperature inside the unit.

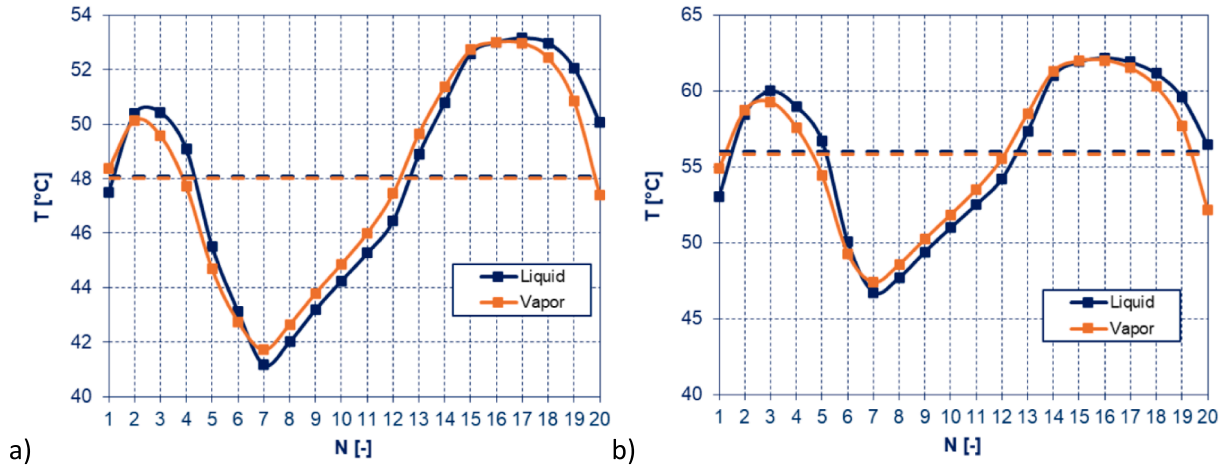

Fig. 19. Temperature profiles for the isothermal absorber. a) $P = 80$ bar; b) $P = 100$ bar. The horizontal dashed lines represent the mean temperature inside the unit.

the single-stage configuration of the reaction section, the process turns out to be more effective than the traditional layout both from the thermal and electric energy requirements. As for the two-stage reactor, the difference between the two processes becomes lower.

The two-stage isothermal absorber at 80 bar is able to provide the minimum ϕ for the absorption-enhanced Haber-Bosch process and can

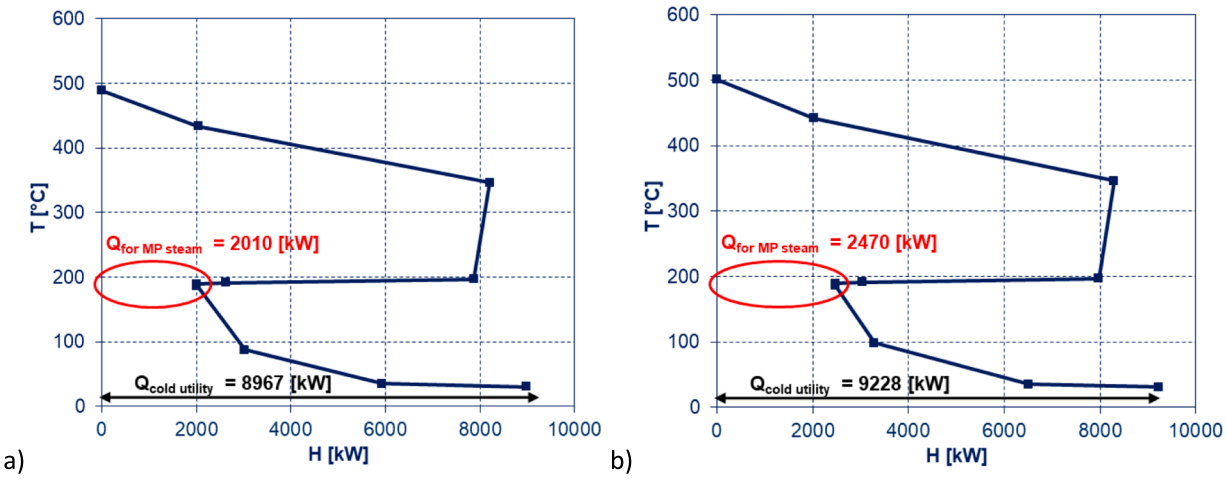

Fig. 20. Grand composite curves of the two-stage absorption-enhanced Haber-Bosch with isothermal absorber. a) $P = 80$ bar; b) $P = 100$ bar.

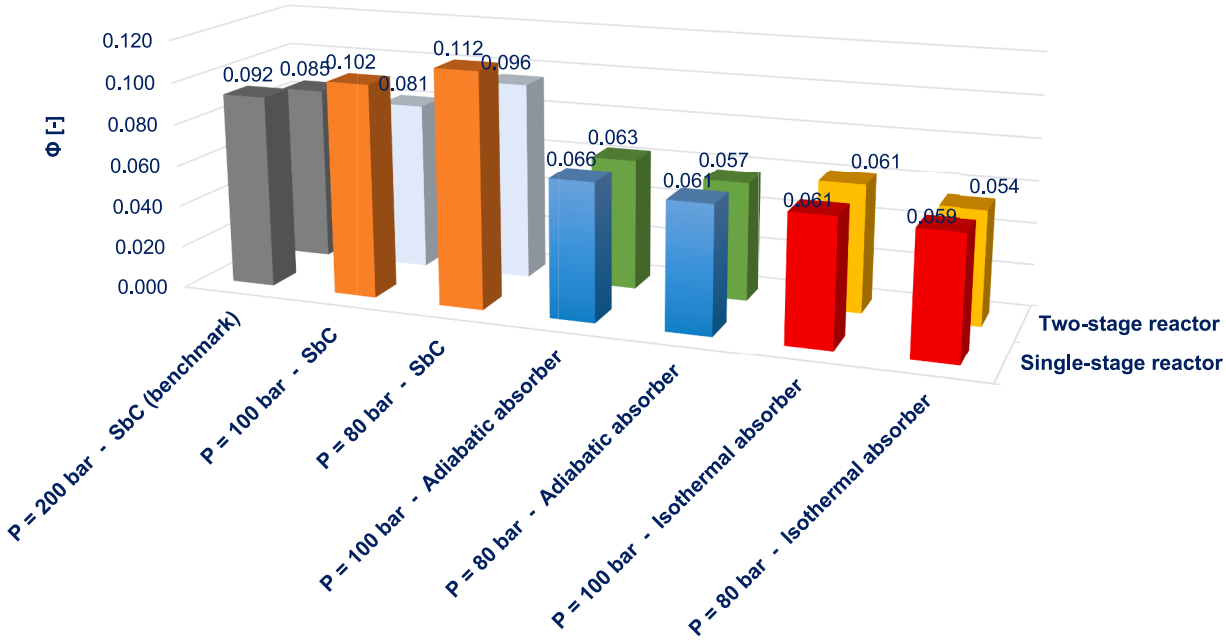

Fig. 21. Results of the NH_3 equivalent analysis. Autothermal absorption-enhanced Haber-Bosch scenarios compared to the conventional process ("SbC").

be considered competitive with respect to the conventional process operated at the same pressure (80 bar). These low pressures enable to accommodate the flexibility demanded by renewable energy.

This promising performance establishes a foundation for a more comprehensive process analysis, which will encompass an exergy evaluation of all equipment to identify sources of inefficiency, as well as an economic assessment that accounts for both fixed and operating expenditures.

5. Conclusions

Ammonia process intensification on a small scale is a critical advancement in addressing modern energy and sustainability challenges. The scaling down of the production enables the processes to respond dynamically to variable energy inputs, such as those from renewable sources like solar or wind. The shift from large-scale concentrated to small-scale distributed NH_3 production is essential for meeting global ammonia demand while minimizing environmental impacts, paving the way for a sustainable and resilient future.

To support distributed energy systems, optimizing processes to operate effectively at reduced scales is required. To this aim, the feasibility of a novel absorption-enhanced Haber Bosch process is demonstrated in this work and its performance is assessed. Then, the base-case absorption-enhanced Haber-Bosch configuration is optimized from the energy point of view, with the aid of pinch analysis and NH_3 equivalent emissions evaluation. In the single-stage configuration of the reaction section, the process turns out to be more effective than the traditional layout both from the thermal and electric energy requirements. To verify if conversion can be further improved, the possibility of applying a two-stage reactor configuration has been explored. Also, the possibility of performing absorption isothermally has been preliminarily investigated.

These promising results pave the way for a novel absorption-enhanced Haber-Bosch technology, which aligns perfectly with current trends in green ammonia production, addressing both energy demands and environmental concerns.

CRediT authorship contribution statement

Elvira Spatolisano: Writing – review & editing, Writing – original draft, Validation, Supervision, Methodology, Conceptualization. **Davide Figini:** Writing – original draft, Software, Investigation.

Declaration of competing interest

The authors declare that they have no known competing financial interests or personal relationships that could have appeared to influence the work reported in this paper.

Appendix A. Supplementary data

Supplementary data to this article can be found online at https://doi.org/10.1016/j.enconman.2025.119904.

Data availability

Data will be made available on request.

References

[1] Pfromm PH. Towards sustainable agriculture: fossil-free ammonia. J Renewable Sustainable Energy 2017;9.
[2] Wang M, et al. Can sustainable ammonia synthesis pathways compete with fossil-fuel based Haber–Bosch processes? Energ Environ Sci 2021;14:2535–48.
[3] Smith C, Hill AK, Torrente-Murciano L. Current and future role of Haber-Bosch ammonia in a carbon-free energy landscape. Energ Environ Sci 2020;13:331–44.
[4] I.P. Hub, Ammonia, Nitrogen, and Green Hydrogen Production & Purification, Deutsche Gesellschaft für Internationale Zusammenarbeit (GIZ) GmbH, Berlin, 2024.
[5] Spatolisano E, Pellegrini LA. Haber-Bosch process intensification: a first step towards small-scale distributed ammonia production. Chem Eng Res Des 2023;195:651–61.
[6] Lin B, Nowrin FH, Rosenthal JJ, Bhown AS, Malmali M. Perspective on intensification of haber−bosch to enable ammonia production under milder conditions. ACS Sustain Chem Eng 2023;11:9880–99.
[7] Richard S, et al. Power-to-ammonia synthesis process with membrane reactors: technoeconomic. Int J Hydrogen Energy 2024;73:462–74.
[8] Wakimoto K, et al. Green ammonia production via recycle membrane reactor: experiment and process simulation. Chem Eng J 2024.
[9] Liu CY, Aika K-I. Ammonia absorption into alkaline earth metal halide mixtures as an ammonia storage material. Industrial & Eng Chem Res 2004;43:7484–91.
[10] Huberty MS, Wagner AL, McCormick A, Cussler E. Ammonia absorption at haber bosch process conditions. AlChE 2012;58:3526–32.
[11] Malmali M, Wei Y, McCormick A, Cussler EL. Ammonia synthesis at reduced pressure via reactive separation. Ind Eng Chem Res 2016;55:8922–32.
[12] Smith C, Malmali M, Liu C-Y, McCormick AV, Cussler EL. Rates of ammonia absorption and release in calcium chloride. ACS Sustain Chem Eng 2018;6:11827–35.
[13] Ojha DK, et al. Integrated ammonia synthesis and separation. ACS Sustain Chem Eng 2019;7:18785–92.
[14] Kale MJ, et al. Optimizing ammonia separation via reactive absorption for sustainable ammonia synthesis. ACS Appl Energy Mater 2020;3:2576–84.
[15] Smith C, McCormick AV, Cussler EL. Optimizing the conditions for ammonia production using absorption. ACS Sustain Chem Eng 2019;7:4019–29.
[16] Malmali M, Le G, Hendrickson J, Prince J, McCormick AV, Cussler EL. Better absorbents for ammonia separation. ACS Sustain Chem Eng 2018;6:6536–46.
[17] Wagner K, et al. Column absorption for reproducible cyclic separation in small scale ammonia synthesis. AlChE J 2017;63:3058–68.
[18] Ammonia, Ullmann's Encyclopedia of Industrial Chemistry, John Wiley & Sons, Ltd2006.
[19] G. Pagani, U. Zardi New separation process gives cheaper ammonia, Hydrocarbon Processing 51 (1972) 106-110.
[20] Perry RH, Green DW. Perry's chemical engineers' handbook. New York: McGraw Hill; 2008.
[21] M. Guadalupi, Process for treating gases in the ammonia synthesis, United States of America, 1977.
[22] Saviano F, Laganà V, Bisi P. Integrate recovery systems for low energy ammonia production. Hydrocarb Process 1981;60:99–110.
[23] A.L. Kohl, R.B. Nielsen, Removal and Use of Ammonia in Gas Purification, in: 5th (Ed.) Gas Purification, Gulf Professional Publishing, Houston, 1997, pp. 278-329.
[24] Moulijin JA, Makkee M, Van Diepen AE. Chemical Process Technology. Chichester: Wiley; 2013.
[25] Topsøe, KM1 and KM1R - Ammonia synthesis catalysts.
[26] Nielsen A, Kjaer J, Hansen B. Rate equation and mechanism of ammonia synthesis at industrial conditions. J Catal 1964;3:68–79.
[27] Elnashaie S, Abashar ME, Al-Ubaid A. Simulation and optimization of an industrial ammonia reactor. Ind Eng Chem Res 1988;27:2015–22.
[28] Dyson DC, Simon JM. Kinetic expression with diffusion correction for ammonia synthesis on industrial catalyst. Ind Eng Chem Fundam 1968;7:605–10.
[29] S.M. Walas, Chemical process equipment: Selection and Design, Butterworth-Heinemann, Oxford, 1988.
[30] Mok L. Sensitivity study of energy consumption. Massachussets Institute of Technol 1980.
[31] Pernicone N, et al. Wustite as a new precursor of industrial ammonia synthesis catalysts. Appl Catal A 2003;251:121–9.
[32] Spatolisano E, Pellegrini LA. CO_2-tolerant cryogenic nitrogen rejection schemes: analysis of their performances. Ind Eng Chem Res 2021;60:4420–9.
[33] AspenTech, Aspen Plus®, Burlington (MA), United States, (2019).
[34] E.E. Ludwig, Applied process design for chemical and petrochemical plants, 3rd ed.1994.